Photoconductivity of Silicon Naphthalocyanine Thin Films

Shigeru Hayashida and Nobuyuki Hayashi*

Ibaraki Research Laboratory, Hitachi Chemical Co. Ltd., Hitachi, Ibaraki 317 Japan

Received May 4, 1990

The relative photocurrent quantum efficiencies of four silicon naphthalocyanine compounds in vacuum-deposited thin films were found to depend on the axial substituents bonded to the central metal silicon. Electronic, infrared, fluorescence, and photoacoustic spectroscopies, together with measurements of short-circuit photocurrent and low-frequency capacitance, were used in combination to investigate the photoelectrical activity and to elucidate the mechanism of photocarrier generation. There appears to be competition between photocarrier generation and nonradiative decay. In addition, the relative photocurrent quantum efficiency appears to be governed by (i) the degree of stacking of naphthalocyanine molecules in the thin films, (ii) the lattice relaxation originating from the vibrational and rotational motions of axial substituents bound to silicon, and (iii) the local electric field at the interface between aluminum substrate and the silicon naphthalocyanine thin films.

Introduction

There has been considerable interest in recent years in the physical and chemical properties of phthalocyanines (Pcs). This interest stems in part from their possible application in areas such as electrophotography,[1] liquid crystals,[2] conductive polymers,[3] electrochromic displays,[4] and photoelectrochemical energy conversion.[5]

Our interest concerns the application of Pcs as charge-generating materials for photoreceptors active in the near-infrared region. Most Pcs possess insufficient absorption in the near-infrared region where solid-state GaAs lasers operate. This problem has, however, been successfully solved by treating the sample with vapor or solvent[6] or milling,[7] which causes a spectral shift or enhancement of the absorption. The mechanism of the spectral shift, particularly with respect to its driving force, is not yet fully understood. Another possible method to produce a new absorption maxima in the near-infrared region is to use molecules having greater conjugation, such as naphthalocyanines (Ncs), rather than Pcs. The absorption spectra of Ncs have already been reported by Kenney et al.[8]

This paper reports on the electronic absorption and short-circuit photocurrent action spectra of four silicon naphthalocyanine (SiNc) compounds in vacuum-deposited thin films. The mechanism of carrier generation was characterized by fluorescence emission and photoacoustic spectroscopy (PAS). Finally, the electrical properties at the Al|SiNC interface of an Al|SiNc|NESA sandwich cell were measured by the low-frequency capacitance method.[9,10]

Experimental Section

Four silicon naphthalocyanine compounds were synthesized according to the procedure of Kenney.[8] The alkyl chains of trialkylsiloxy groups, as axial substituents of SiNcs, were varied from ethyl to hexyl, as shown in Figure 1. All the SiNcs were purified by recrystallization from chloroform.[11]

Table I. Red Shifts ($\Delta\lambda$) and Fwhm (ΔW) of Each SiNc Thin Film in the Q-Band Absorption

compd	$\Delta\lambda$	ΔW
1	48	72
2	38	60
3	35	54
4	27	38

NESA glass with a sheet resistance of 10—20 Ω/□ was used as a substrate in this study. The Al|SiNc|NESA cells were prepared by conventional vacuum deposition. Each SiNc compound was evaporated from a Mo crucible onto NESA glass kept at ambient temperature under a chamber pressure of 4×10^{-4} Pa. The crucible temperature was kept at 470 °C for compound 1, 410 °C for compound 2, 370 °C for compound 3, and 350 °C for compound 4. The thickness of each SiNc film was 0.3–0.35 μm. The top layer Al electrode was vacuum deposited to a thickness of 30 nm.

The short-circuit photocurrent action spectra for the Al|SiNc|NESA sandwich cells were measured with a lock-in amplifier/preamplifier (NF Electronic Instrument LI-570/LI-76), light chopper, 300-W halogen lamp, and monochromator. The incident light beam was modulated at a frequency of 80 Hz. The cells were irradiated through the Al electrode. The transmissions of Al films were almost 1% in the visible and near-infrared region.

The photoacoustic spectra (PAS) were measured with the same equipment as the short-circuit photocurrent measurement except for the addition of an EGG PARC Model 6003 photoacoustic cell. To confirm the reproducibility, several experiments were carried out.

The capacitance was measured by using a low-frequency capacitance method reported by Twarowski[9] and Loutfy.[10] A triangular voltage waveform with a frequency of 0.2 Hz and voltage of 1.0 V was applied to the Al|SiNc|NESA cells by using a Hokuto polarographic wave generator and analyzer, Models HA-501 and HB-104, respectively.

The electronic and fluorescence spectra of the SiNcs were measured on a Hitachi 3400 spectrophotometer and a Hitachi 850 fluorescence spectrometer, respectively. The radiative lifetime (τ) of each SiNc was determined with a HORIBA time-resolved spectrofluorometer, NAES-1100.

(1) Loutfy, R. O.; Hor, A. M.; Rucklidge, A. *J. Imag. Sci.* **1987**, *31*, 31. Byrne, J. F.; Kurz, P. F. U.S. Patent 3,357,989, 1967.
(2) Belarbi, Z.; Sirlin, C.; Simon, J.; Andre, J.-J. *J. Phys. Chem.* **1989**, *93*, 8105.
(3) Hanack, M. *Mol. Cryst. Liq. Cryst.* **1988**, *160*, 133.
(4) Castaneda, F.; Plichon, V.; Clarisse, C.; Riou, M. T. *J. Electronal. Chem.* **1987**, *233*, 77.
(5) Sims, T. D.; Pemberton, J. E.; Lee, P.; Armstrong, N. R. *Chem. Mater.* **1989**, *1*, 26.
(6) Iwatsu, F.; Kobayashi, T.; Ueda, N. *J. Phys. Chem.* **1980**, *84*, 3223.
(7) Kakuta, A.; Mori, Y.; Takano, S.; Sawada, M.; Shibuya, I. *J. Imag. Technol.* **1985**, *11*, 7.
(8) Wheeler, B. L.; Nagasubramanian, G.; Bard, A. J.; Schechtman, L. A.; Dininny, D. R.; Kenney, M. E. *J. Am. Chem. Soc.* **1984**, *106*, 7404.
(9) Twarowski, A. J.; Albrecht, A. C. *J. Chem. Phys.* **1979**, *70*, 2255.
(10) Shing, Y. H.; Loutfy, R. O. *J. Appl. Phys.* **1981**, *52*, 6961.

(11) $C_{60}H_{54}N_8O_2Si_3$ (1) mp >300 °C. Anal. Calcd; 11.17% N, 71.82% C, 5.42% H. Found: 10.92% N, 70.45% C, 5.34 H. ^{1}H NMR ($CDCl_3$) δ −2.07 (q, 18 H, J = 7.93 Hz), −1.02 (t, 12 H, J = 7.93 Hz), 7.93 (dd, 8 H, J = 6.10 and 3.05 Hz), 8.68 (dd, 8 H, J = 6.10 and 3.05 Hz), 10.13 (s, 8 H). $C_{66}H_{66}N_8O_2Si_3$ (2) mp 300 °C. Anal. Calcd: 10.30% N, 72.89% C, 6.12% H. Found: 10.28% N, 72.70% C, 6.13% H. ^{1}H NMR δ −2.06 (t, 12 H, J = 7.32 Hz), −0.85 (sextet, 12 H, J = 7.32 Hz), −0.28 (t, 18 H, J = 7.32 Hz), 7.93 (dd, 8 H, J = 6.10 and 3.35 Hz), 8.68 (dd, 8 H, J = 6.10 and 3.35 Hz), 10.03 (s, 8 H).

0897-4756/91/2803-0092$02.50/0

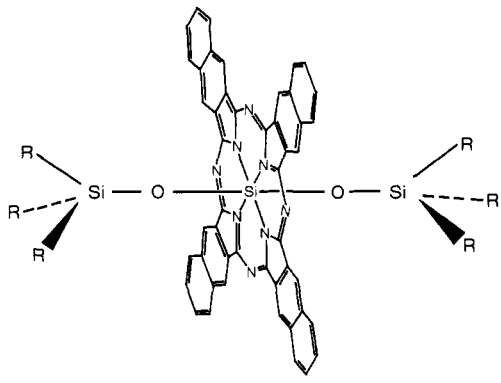

Figure 1. Molecular structure of SiNc: **1**, R = C_2H_5; **2**, R = n-C_3H_7; **3**, R = n-C_4H_9; **4**, R = n-C_6H_{13}.

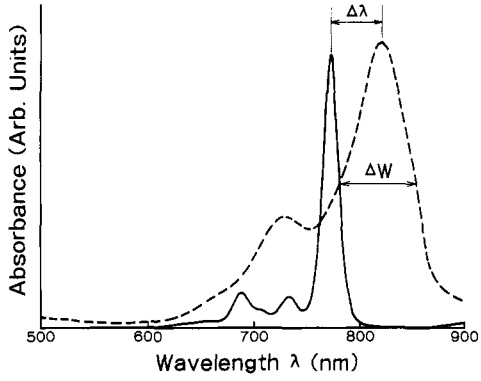

Figure 2. Absorption spectra of 1 in solution (solid line) and in the vacuum-deposited thin film (dashed line).

Results and Discussion

Electronic Absorption Spectra. Figure 2 (solid curve) shows the absorption spectrum of compound **1** in the Q-band region (500–900 nm) in methylene chloride. The absorptions in solution were sharp and intense (λ_{max} = 773 nm and $\epsilon = 8 \times 10^5$ M^{-1} cm^{-1}). The λ_{max} and the ϵ values of compounds **2–4** were almost the same as those of compound **1** and coincided with those of compound **4** reported by Kenney,[8] who showed that the λ_{max} and ϵ values of compound **4** were 772 nm and 4×10^5 M^{-1} cm^{-1}, respectively. As shown in Figure 2 (dashed curve), the λ_{max} in the vacuum-deposited thin film of compound **1** shifted considerably to the red region from that in solution. The absorption spectra in the vacuum-deposited thin films of compounds **2–4** also resembled that of compound **1**. However, the λ_{max}'s and band widths of absorptions of compounds **1–4** in the thin films depended on the axial substituents of the SiNcs. As shown in Table I, the red-shift ($\Delta\lambda$) and full width at half-maximum (fwhm, ΔW) of the Q-band absorption decrease as the length of the alkyl chain in the axial substituents increased. The red-shift and/or splitting of the Q-band of various Pcs have been previously reported for vacuum-deposited and ball-millground dispersion films.[12] According to Davydov's theory,[13] the Q-band splits into as many components as there are nontranslationally equivalent molecules in the unit cell, and the amount of splitting depends on the interaction energy between molecules with different site symmetries. The splitting of the Q-band was not observed

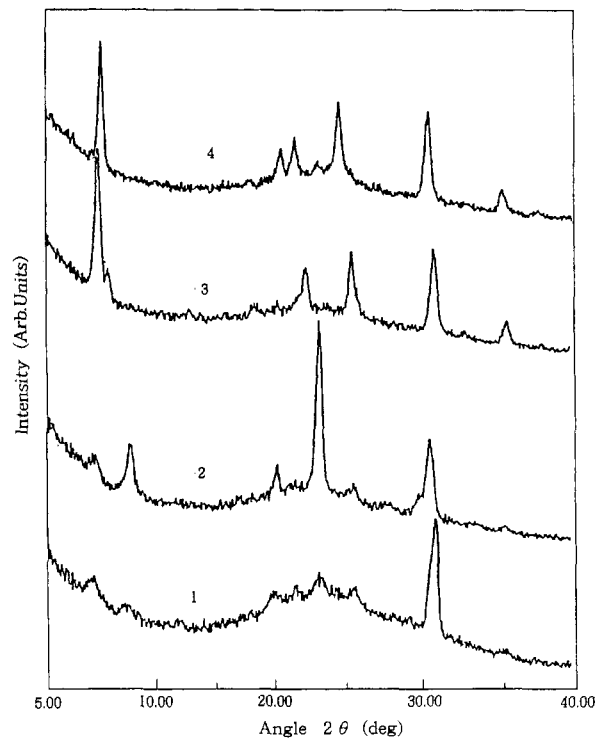

Figure 3. X-ray diffraction patterns of SiNcs in the vaccum-deposited thin films.

in the present vacuum-deposited thin films. This finding suggests that all of the SiNcs are translationally equivalent in the thin films. While it is known that the red-shift of the Q-band is sensitive to stacking arrangements of Pc molecules in the thin films,[5] the cofacial stacking generally observed with various Pcs appears to be limited by steric hinderance due to two bulky trialkylsiloxy groups that are axially linked to the central metal silicon of SiNcs. The observed red-shifts of compounds **1–4** in the vacuum-deposited thin films, however, were quite large and dependent on the length of the alkyl chain in the axial substituents. The results suggest that the spectral changes of compounds **1–4** in the vacuum-deposited thin films relative to those in solution are attributable to the stacking arrangement of naphthalocyanine molecules originating from the difference of aggregation. This aggregation is caused by an intermolecular interaction between adjacent chromophores[14] that appeared to increase according to the following order: **4** < **3** < **2** < **1**. Figure 3 shows the X-ray diffraction patterns of the present vaccum-deposited thin films. Relatively sharp diffraction lines at d spacings from 2.9 to 4.4 Å are observed. The observed crystallinity suggests that naphthalocyanine molecules must be packed in an orderly fashion in the thin films. X-ray diffraction studies on halide-bridged gallium, aluminum, or indium Pcs show strong reflections in the region corresponding to the interplanar spacings of 3.3–3.8 Å.[15] A recent single-crystal study of a slipped-cofacial stacked GaPc–Cl structure also showed a 3.34-Å interplanar spacing.[16] From these data, we tentatively propose assignment of the interplanar spacings of compounds **1–4** to 3.49, 3.50, 3.54, and 3.63 Å, respectively. This result and the observed red-shifts as described above suggest that the intermole-

(12) (a) Griffiths, C. H. *Mol. Cryst. Liq. Cryst.* **1979**, *33*, 149. (b) Sharp, J. H.; Lardon, J. *J. Phys. Chem.* **1968**, *72*, 3230. (c) Kobayashi, T. *Spectrochim. Acta, Part A* **1970**, *26*, 1313. (d) Loutfy, R. O.; Hor, A. M.; DiPaola-Baranyi, G.; Hsiao, C. K. *J. Imag. Sci.* **1985**, *29*, 116.

(13) Davydov, A. S. *Theory of Molecular Excitations*; Kasha, M., Oppenheimer, Jr., M. Ed.; McGraw-Hill: New York, 1962.

(14) Law, K.-Y.; Chen, C. C. *J. Phys. Chem.* **1989**, *93*, 2533.

(15) (a) Nohr, R. S.; Kuznesof, P. M.; Wynne, K. T.; Kenny, M. E.; Siebemann, P. C. *J. Am. Chem. Soc.* **1981**, *103*, 4371. (b) Lincky, J. P.; Paul, T. R.; Nohr, R. S.; Kenny, M. E. *Inorg. Chem.* **1980**, *19*, 3131. (c) Nohr, R. S.; Wynne, K. J. *J. Chem. Soc., Chem. Commun.* **1981**, 1210.

(16) Wynne, K. J. *Inorg. Chem.* **1984**, *23*, 4658.

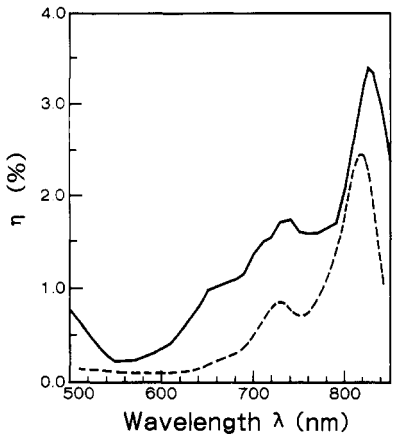

Figure 4. Absorption (dashed line) and action spectra (solid line) of **3** in the vacuum-deposited thin films.

Table II. Relative Photocurrent Quantum Efficiency (η) of SiNcs under Illumination at 800 nm

compd	η, %	compd	η, %
1	6.36	3	2.05
2	2.46	4	0.07

cular interaction of naphthalocyanine molecules in the thin films decreases with the increase of the alkyl chain length in the axial substituents. Single-crystal analyses are in progress to explain the relationship between the aggregation and physical properties of naphthalocyanine molecules.

Photoconductivity. Figure 4 (solid curve) shows a typical action spectrum of compound **3**, which was obtained by measuring the short-circuit photocurrent as a function of excitation wavelength. The relative photocurrent quantum efficiency, η, can be calculated from the photocurrent generated under monochromatic illumination at low incident light levels:

$$\eta = \frac{1.24 J_{ph}\ (A/cm^2)}{I\ (W/cm^2) \times \lambda\ (\mu m)} \quad (1)$$

where I, λ, and J_{ph} represent the incident light intensity, the wavelength of the incident light, and the short-circuit photocurrent, respectively. The relative photocurrent quantum efficiencies of compounds **1**–**4** at 800 nm, obtained by using eq 1 in vacuum-deposited thin films are given in Table II. Compound **1** was the most photoactive material in this series. The relative photocurrent quantum efficiencies increased as the length of the alkyl chain in the axial substituents decreased, as seen in Table II. This result clearly demonstrates the dependence of the photoelectrical properties of SiNcs on the molecular structures and morphological properties.[17]

The absorption spectrum of compound **3** in the vacuum-deposited thin film is also given in Figure 4 (dashed curve). The action spectrum coincides with the absorption spectrum. The action spectra of compounds **1**, **2**, and **4** were also similar to their absorption spectra. On the other hand, it is known that the action spectra of anthracene and azulene derivatives have strong wavelength dependencies. Their relative photocurrent quantum efficiencies increase with increased photon energy.[18] Since the intramolecular relaxation of anthracene and azulene derivatives from an upper excited state to the lowest excited state (the first excited singlet state) is relatively slow, the excess energy

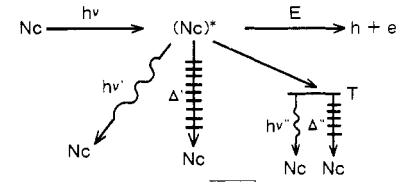

Figure 5. Schematic representation of the model used to explain photocarrier generation and decays.

Table III. Fluorescence Quantum Efficiency (ϕ) and Lifetime (τ) of SiNcs

compd	ϕ, %	τ, ns
1	0.21	4.1
2	0.31	4.3
3	0.09	4.3
4	0.13	4.3

stored in the upper excited states results in a large electron–hole pair thermalization separation distance. Therefore, the probability of the electron–hole pair dissociation to free carriers increases. However, the present results differ from those of anthracene and azulene derivatives. The fact that the action and absorption spectra coincide indicates that the first excited singlet state of SiNcs participates in photocarrier generation. It does not, however, allow one to determine whether this state is the immediate precursor to the photocarrier generation or whether another state, such as the lowest triplet state populated via intersystem crossing from the first excited singlet state, is the direct photocarrier generation precursor.

The photocarrier generation model is described schematically in Figure 5, where Nc*, T, and Nc denote the first exicted singlet, lowest triplet, and ground states of SiNc, respectively. SiNc is excited to a higher state by an incident photon and thermalizes to the first excited singlet state by internal conversion, where the excited SiNc decays to the ground state, Nc, radiatively giving rise to fluorescence and/or nonradiatively producing instantaneous heat. Furthermore, it can decay to the lowest triplet state by intersystem crossing, and from the state it can further return to the ground state by radiative and nonradiative decays. In this study, we ignored the carrier generation from the lowest triplet state because the observed photocurrents of compounds **1**–**4** are likely to be due mainly to the carrier generated from the first excited singlet states according to the paper of Firey,[19] where the reported quantum yield of the triplet of compound **4** is 0.2. In this carrier-generation model, the photocarrier generation competes with radiative and nonradiative decays from the first excited singlet state. In other words, the more the photocarrier generation, the less the radiative and nonradiative decays. Correlation between photocarrier generation and radiative decay was quantitatively investigated by electrich-field-induced fluorescence measurements according to a method by Menzel and Popovic.[20] The dependence of photocarrier generation on nonradiative decay was, in turn, estimated by measuring the photoacoustic signal produced by applying an electric field to the sample.[21]

The fluorescence spectra of compounds **1**–**4** measured in the vacuum-deposited thin films were very weak and independent of the alkyl chain in the axial substituents. The fluorescence quantum efficiencies, ϕ, of compounds

(17) Law, K.-Y. *J. Phys. Chem.* **1988**, *92*, 4226.
(18) Hong, M.; Noolandi, J. *J. Chem. Phys.* **1979**, *70*, 3230.
(19) Firey, P. A.; Ford, W. E.; Sounik, J. R.; Kenny, M. E.; Rodgers, M. A. J. *J. Am. Chem. Soc.* **1988**, *110*, 7626.
(20) Menzel, E. R.; Popovic, Z. D. *Chem. Phys. Lett.* **1978**, *55*, 177.
(21) Tam, A. C. *Appl. Phys. Lett.* **1980**, *37*, 978.

Table IV. PAS Intensity Q of SiNcs

compd	Q, μV	compd	Q, μV
1	4.8	3	5.7
2	5.8	4	6.8

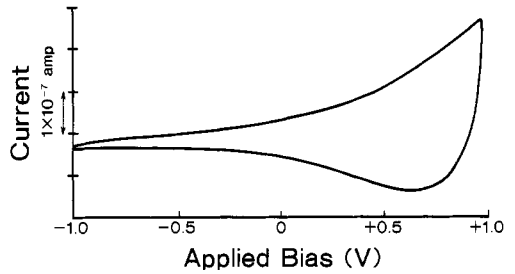

Figure 6. Current–voltage trace of an Al|SiNc|NESA sandwich cell under 800-nm illumination.

1–4 in CH_2Cl_2 solution, which were normalized by quinine sulfate, were also very low, as shown in Table III. These values were also independent of the alkyl chain in the axial substituents. The lifetimes of the fluorescence are also given in Table III. The lifetimes of compounds 1–4 were almost identical. These results indicate that there is no correlation between the fluorescence and the molecular structure, namely, the length of the alkyl chain in the axial substituents of the SiNcs. This finding suggests that the radiative decay does not appear to be important in the present carrier generation model.

It may be concluded that the photocarrier generation and nonradiative decay are the only two competing processes from the results of the fluorescence measurements. In these processes, an increase in photocarrier generation leads to a decrease of heat production, which is derived from nonradiative decay, and hence a decrease in the PAS intensity (Q). The PAS intensities of compounds 1–4 are shown in Table IV. They had a tendency to decrease as the length of the alkyl chain in the axial substituents decreased, except that the PAS intensity of compound 3 was almost the same as that of the compound 2. The dependence of Q on the alkyl chain of the axial substituents suggests that PAS intensities may represent the extent of lattice relaxation originating from the vibrational and rotational motions of alkyl chains of the axial substituents. Thus we have shown that the relative photocurrent quantum efficiencies increase as the length of the alkyl chain increases. These results support the model that the photocarrier generation and nonradiative decay are two competing processes.

Finally, the electric properties of the Al|SiNc interface of Al|SiNc|NESA sandwich cells were investigated in terms of the capacitance–voltage characteristic by using a low-frequency capacitance method.[9,10] A typical current–voltage trace for an Al|SiNc|NESA sandwich cell under illumination is shown in Figure 6. The horizontal axis from left to right was swept from the reverse to the forward bias voltage. The vertical axis indicates the current flow through the sandwich cell. The currents, i_1 and i_2, at a given potential were determined from the upper and lower traces, respectively. The capacitance as a function of the applied bias was then determined by eq 2, where V_0 is the

$$C(V) = \frac{i_1 - i_2}{8V_0\nu} \qquad (2)$$

amplitude of a triangular voltage and ν is the frequency. Table V is a summary of the values for the Schottky depletion layer width at zero applied bias, the carrier concentration, the barrier potential, and the local electric field, which was calculated from the depletion layer width and the barrier potential, all obtained from analyses of linear $1/C^2$ vs V plots for SiNc sandwich cells. A values of 3.2 was used for the dielectric constant of SiNc. We could not obtain the capacitance from the sandwich cell of compound 4 because the values of i_1 and i_2 were almost identical. This result indicates that there was no Schottky barrier at the interface between Al and the thin film of compound 4. The magnitude of the local electric field, E, depended on the alkyl chain of the axial substituents, which increased as the length of alkyl chain decreased. The relative photocurrent quantum efficiency is also given in Table V. Loutfy has shown that the charge-carrier generation in organic solar cells is almost completely limited to the depletion region because the electric field is required to assist the carrier generation.[22] Our finding that the photocurrent quantum efficiency increased as the magnitude of the local electric field increased supports his results.

Table V. Parameters of the Schottky Depletion Layer

compd	depletion width, Å	carrier concn, m^{-3}	barrier potential, V	10^{-5} × local electric field, V/cm	η, %
1	140	87.5	0.47	3.36	6.36
2	950	1.99	0.50	0.53	2.46
3	1300	1.29	0.60	0.46	2.05
4					0.07

Conclusions

The Q-band absorptions of SiNcs in vacuum-deposited thin films were found to red-shift compared with those in solution. The shift increased as the length of alkyl chain in the axial substituents decreased. This result suggests that there is a weak intermolecular interaction between adjacent chromophores of SiNcs in the vacuum-deposited thin films.

The estimated relative photocurrent quantum efficiencies of SiNcs in the vacuum-deposited thin films increased as the length of alkyl chain in the axial substituents decreased. The fluorescence quantum efficiencies of the SiNcs showed no correlation between photocarrier generation and radiative decay. Thus the nonradiative decay appeared to compete with the photocarrier generation since the magnitude of photoacoustic signals of the SiNcs depended on the alkyl chain in the axial substituents and decreased as the length of alkyl chain decreased.

The electrical properties of each Al|SiNc interface were determined by a low-frequency capacitance method. The estimated local electric field at the Al|SiNc interface was found to be strongly dependent on the alkyl chain in the axial substituents.

We propose that the relative photocurrent quantum efficiency of each SiNc is governed by (i) the degree of the stacking of each SiNc in vacuum-deposited thin films, (ii) the degree of the lattice relaxation originating from the vibrational and rotational motions of the axial substituents of each SiNc in the vacuum-deposited thin films, and (iii) the magnitude of the local electric field at each Al|SiNc interface.

Acknowledgment. We are grateful to Dr. S. Tai for synthesizing the silicon naphthalocyanines and thank Dr. T. Okamoto for his helpful comments.

Registry No. 1, 115501-72-9; 2, 115501-73-0; 3, 115501-74-1; 4, 92396-88-8.

(22) Loutfy, R. O.; Sharp, J. H. *J. Chem. Phys.* **1979**, *71*, 1211.